Supporting Information

SI Materials and Methods

Bacterial culture conditions

All bacterial strains used in this study are listed in SI Appendix, Table S1. *Escherichia coli* were grown in Luria-Bertani (LB; Oxoid) broth with desired antibiotics. *Staphylococcus aureus* strains were grown in Trypticase soy agar (TSA), Trypticase soy broth supplemented with glucose (TSB + Glc) (0.25%, wt/vol), B2 medium (1% casein hydrolysate, 2.5% yeast extract, 2.5% NaCl, 0.1% K_2HPO_4, and 0.5% glucose [wt/vol]) with appropriate antibiotics wherever needed. For generation of pooled mutant libraries, *S. aureus* 6850 was grown in Nutrient Broth (NB). For hemolysis analysis *S. aureus* were grown in Blood agar plates made with Columbia agar base (BD Biosciences) supplemented with 5% defibrinated Sheep blood (Fiebig Nährstofftechnik, Germany).

Selection of clinical isolates of *S. aureus* was done on SASelect agar (BioRad) and subculture was done on Horse Blood agar (Oxoid) and for blood cultures the BD Bactec Instrumented Blood culture system (BD Biosciences) was used (see below).

All isolates, whether used for RNA-seq or for *in vivo* challenge, were inoculated into tryptic soy broth (TSB, Oxoid) and incubated in air overnight at 37°C, 180 rpm.

Generation of mutants in *Staphylococcus aureus* by allelic replacement

Markerless targeted gene deletions were generated as previously described(1). Briefly, approx. 1kb regions flanking the target open reading frame, RSAU_002217, were amplified by PCR (oligonucleotides attB1-2217-up-F and 2217-up-R-SacII as well as 2217-down-F-SacII and attB2-2217-down-R, respectively). The PCR products were joined by SacII restriction and subsequent ligation resulting in a fragment flanked by Gateway® compatible *att*B1 and *att*B2 sites. The fragment was

inserted into pKOR1(1) by incubation with BP clonase (Invitrogen) according to the manufacturer's instructions. The mixture was transformed into *E. coli* TOP10F' (Invitrogen), plated, recombinant plasmids were isolated and confirmed by Sanger sequencing (SeqLab, Göttingen). Subsequently, the replacement vector was electroporated into *S. aureus* RN4220 (2), a restriction-deficient and methylation-proficient strain which accepts foreign DNA. Recombinant *S. aureus* was grown in Tryptone Soy Broth (TSB) containing 10 µg/ml chloramphenicol (Cam) at 30°C, plasmids were purified, and electroporated into the *S. aureus* target strain(2). The bacteria were plated on TSA/Cam overnight at 30 °C. Recombinant bacteria were inoculated in TSB/Cam and grown overnight at 43°C. Subsequently, dilutions of the culture were streaked on Tryptone Soy Agar (TSA)/Cam and incubated overnight at 43°C. At these temperatures, the thermo-sensitive origin of replication within pKOR1 does not allow plasmid replication and thus co-integrates within the genome are formed by homologous recombination. Multiple resulting colonies were inoculated and grown in antibiotic-free TSB at 30°C, thus allowing for co-integrate resolution. The cultures were diluted 1:10,000, plated on TSA containing 100 ng/ml anhydrotetracycline and grown at 37°C thereby counter-selecting for the presence of the plasmid backbone(1). Resulting colonies were inoculated and grown overnight in TSB at 37°C. Genomic DNA was isolated and successful gene deletion was determined by PCR using oligonucleotides 2217_test_F and 2217_test_R (SI Appendix, Table S3).

Construction of plasmid pS2217 for *in trans* complementation in *Staphylococcus aureus*

The plasmid pS2217 was generated to complement *rsp* gene *in trans* under the transcriptional control of its native promoter. Briefly, the open reading frame of *rsp* gene (*S. aureus* 6850 locus ID: RSAU_002217) was amplified from *S. aureus* genomic DNA, with its native promoter i.e. 120 bp upstream of gene, with the primers 2217_intpromoter_F_NotI and 2217_intpromoter_R_BamHI (SI Appendix, Table S2). The 2.2 kb insert was archived in pCR2.1 TOPO® TA vector and propagated *E. coli* DH5α, followed by examination by sequencing. The insert was digested out with NotI and BamHI restriction enzymes and ligated to pmRFPmars (3) vector digested with the same set of enzymes, to

create pS2217. The vector was transformed into *E. coli* DH5α and plated on LB agar plates supplemented with Ampicillin. The plasmid pS2217 was isolated form *E. coli* was propagated through *S. aureus* RN4220 and finally transformed into electro-competent *S. aureus* 6850 Δ*rsp* or the insertional mutant USA300 LAC* *rsp*::*erm*B and selected on TSA containing 10 µg/ml chloramphenicol. The resulting strains were grown in TSB at 37°C overnight and stored as glycerol stocks at -80°C.

Gentamicin susceptibility assays

All strains of *S. aureus* were grown overnight in Tryptic Soy Broth (TSB, Oxoid) and diluted to optical density of 0.1 at 600 nm. Bacteria were plated on Muller Hinton (Sigma) agar and gentamicin Etest® MIC (Biomerieux) strips were laid on. The plates were incubated at 37°C for 16-18 hours and the MIC were determined at the concentration on the strip where growth inhibition occurred.

Bacterial clinical samples

Staphylococcus aureus strains were isolated from two patients with concomitant nasal carriage and bloodstream infection. Patient P was recruited to a previously reported longitudinal study of asymptomatic carriage among adults attending general practices in Oxfordshire, United Kingdom, developing a *S. aureus* bloodstream infection 15 months after joining the study (4). Patient S was treated for a *S. aureus* bloodstream infection at a hospital in Oxfordshire, United Kingdom, with a nasal swab subsequently taken as part of routine surveillance. Microbiological processing was as described (4); briefly, nasal swabs were plated on SASelect agar (BioRad) overnight at 37 ºC, and individual colonies were subcultured onto horse blood agar (Oxoid). Blood cultures used the BD Bactec system; media from the positive bottles was plated on horse blood agar, and colonies were picked from each bottle for sequencing. DNA was extracted using a commercial kit (FastDNA, MP Biomedicals), sequenced using Illumina paired end sequencing as described (4). Both de-novo and

mapping based approaches were applied. The *rsp* sequence de novo assembly reads resulting from whole genome sequencing from Patient S nasal (*rsp*$^{+}$) and bloodstream (*rsp*$^{-}$) isolates, were identified using blastn. Protein sequences were obtained from the corresponding DNA sequences using EMBOSS Transeq(5). Alignment with ALIGN_Query(6) was used to compare the predicted protein sequences. The protein sequences found were submitted to the Pfam(7) database for sequence search. The helix-turn-helix domain HTH_18 aligns to amino acid coordinates 169 to 247. No other significant Pfam matches were found.

From patient P we selected for further investigation one nasal culture isolate (isolate reference C1360) and one blood culture isolate taken 394 days later (isolate C1158) that differed by ten variants, including a premature stop codon in the AraC-family transcriptional regulator *rsp* (8). This included two substitutions previously excluded on the grounds that they occur in repetitive regions: a point mutation in tRNA-Lys and a single base deletion upstream of fibronectin binding protein precursor *fnbA*. From patient S we selected for further investigation one nasal isolate (isolate C24365) and one blood isolate (isolate C24366) taken 6 days earlier that differed by a single Alanine to Proline point mutation in the helix-turn-helix domain of *rsp* predicted to disrupt DNA binding of the transcriptional regulator. In both cases the nasal isolates were *rsp* wild type and the blood isolates defective. In addition, we obtained from the Nebraska Transposon Mutant Library wild type (JE2) and *rsp* knockout (NE1304) strains of USA300 FPR3757 (LAC).

Bacterial preparation for *S. aureus* pulmonary infections

Desired *S. aureus* strains were revived from frozen stocks by plating on TSA with appropriate antibiotics whenever required. Colonies were picked and grown in TSB overnight at 37°C with shaking at 180 rpm in air. The overnight culture was transferred into a flask containing 50 ml TSB (OD_{600} 0.05) and incubated for 3.5 hours at 37°C with shaking at 180 rpm in air. The bacteria were harvested by centrifugation at 4°C and resuspended in 20 ml TSB containing 15% glycerol. The

bacterial suspension was divided into 2 ml aliquots and stored at -80°C until use. The bacterial stocks were quantified for CFUs and also titrated for lethal and sub-lethal dosage for infection in mice. For infections bacteria from glycerol stocks were thawed, transferred to pre-warmed 50 ml TSB media and incubated at 37 °C for 30 minutes. The bacteria were washed twice with 1x PBS and resuspended in 1 ml PBS. The optical density at 600 nm was determined and bacterial numbers were assessed by way of comparison with reference growth curves that were established for each strain. Bacteria were diluted to contain the desired number of cfu in 20 µl of PBS and aliquots were plated on TSB agar to confirm cfus.

Bacterial growth curves

S. aureus strains were grown overnight in TSB at 37°C with shaking at 180 rpm in air. The culture was diluted to OD_{600} 0.1 in 400 µL TSB in triplicates and grown up to 20 hours in a 48 micro well plate and absorbance at 600 nm was measured every 15 minutes in an automated fashion by TECAN infinite 200 multimode reader.

***Staphylococcus aureus* TnSeq**

Pooled mariner transposon mutant libraries were generated as previously described (9). For chromosomal DNA preparation bacteria were harvested by centrifugation, resuspended in 200 µL of Tris-Sucrose buffer (10 mM Tris-HCl, pH 7.5; 25% sucrose; 15 µL of EDTA) along with 200 µg/mL RNaseA, and 100 µg/mL Lysostaphin (AMBI, Lawrence, NY, USA) and incubated at 37°C for 30 minutes. 325 µL of TE Buffer, 225 µL of 10 % SDS and 20 µL Proteinase K (20 mg/mL) were added and the mixture was incubated at 55°C for 30 minutes. 150 µL 5 M sodium perchlorate was added followed by 0.5 volume of chloroform-isoamyl alcohol (24:1), the mixture was incubated at room temperature for 1 hour with vigorous agitation (200 rpm). The aqueous phase was collected and DNA was precipitated by adding 1 volume of ice-cold isopropanol, incubation on ice for 30 minutes

and centrifugation at 14,000 rpm for 10 minutes. The resulting pellet was washed with 1 mL of 70% ethanol; DNA was air-dried and dissolved in 200 µL nuclease-free water.

DNA was fragmented by sonication in a volume of 1 ml with Diagenode Bioruptor® (Diagenode SA, Belgium) for 10 cycles (30 sec ON/30 sec OFF) at high power setting (position H) at 4°C. 5 µg of sheared DNA were repaired using the NEBNext®End repair module (NEB), purified with Agencourt® AMPure XP magnetic beads (Beckman Coulter), and eluted into 42 µL of sterile nuclease-free water. DNA fragments within the size range of 200-300 bp were selected with Agencourt® AMPure XP magnetic beads following a previously established procedure (10).

Size-selected fragments were subsequently A-tailed using the NEBNext® dA-Tailing module (NEB), the DNA was re-purified on Agencourt® AMPure XP magnetic beads and eluted into 30 µL of sterile nuclease-free water. Multiplexing adaptors were generated by mixing equimolar concentrations of the oligonucleotides MultiPlex-Y-Adapt_f and MultiPlex-Y-Adapt_r (SI Appendix, Table S2) in 1x Oligo annealing buffer (100 mM Tris-HCl pH 7.5, 10 mM EDTA, 500 mM NaCl), heating to 94°C for 5 minutes followed by a gradual cooling to room temperature. Adaptors were ligated to A-tailed DNA-fragments overnight at 16°C and the DNA was purified with Agencourt® AMPure XP magnetic beads followed by elution into 25 µL of sterile nuclease-free water. Enrichment of DNA fragments containing transposon insertion sites as well as introduction of Illumina barcodes and flow cell specific sequences was performed. In 10 cycles of linear PCR using the oligonucleotide TnSeq-HimarPCR, which recognizes the inverted repeat of the himar1 transposon, we enriched for transposon ends. Thereafter one of the MP-TnSeq_Index oligonucleotides was introduced, which is complementary to the library adaptor sequence and carries a unique 7 nt barcode sequence (SI Appendix, Table S2), and the reaction was continued for another 10 cycles. After purification with AMPure beads, the 3’ and 5’ reactions were mixed to get equimolar ratio and successful incorporation of the required sequences was tested by PCR using IS-Himar-Forward and IS-BC-Reverse (SI Appendix, Table S2). The resulting libraries were sequenced on the Illumina® Hi-Seq 2500

platform (single read, with index read) with the transposon-specific oligonucleotide primer Himar1-Seq (SI Appendix, Table S2). Illumina adapter sequences were removed via cutadapt version 1.2.1 (11) and were checked for the sequence pattern 'CAACCTGT' originating from the transposon mosaic end. Only reads containing that specific sequence with maximally one mismatch or gap and a length of minimum length of 16 nucleotides were used for further analyses. The remaining reads were mapped on the *Staphylococcus aureus* 6850 genome (GenBank accession CP006706) via Bowtie2 version 2.1.0 (12). To identify transposon insertion sites (TIS), the alignment start positions of mapped reads were extracted and each position on the genome, covered by at least one alignment start, was annotated as TIS. We adjusted the genomic position strand-specifically to account for the 1 bp shift of the reads mapping on the plus or minus strand. In summary the library comprised bacteria containing approximately 25,000 unique transposon insertion sites (TIS) evenly distributed across the genome (SI Appendix, Figure S1A).

For the gene-wise analysis of the abundance changes of transposon insertion sites, all reads originating from transposon insertion sites were counted for each gene and TnSeq library. Only sites that were detected at least once in both HeLa replicate passage lines had been included in the statistical regression analysis. To reduce the background noise in the mouse lung infection dataset, only sites with two independent detections have been statistically evaluated. Identification of depleted and enriched mutants was performed via DESeq2 version 1.6.2 (13). The HeLa infection experiment was modelled as a time course experiment including a technical replicate with the input libraries as time point 0. For the mouse lung infection experiment, the 3 output libraries were compared to the input libraries. Genes with very low mean normalized read depth (mnrd) were excluded from analysis; genes with mnrd <4 were excluded in the HeLa experiment, and those with mnrd < 8 were excluded in the *in vivo* experiment. The *p*-values were corrected for multiple testing (14). Genes showing an adjusted *p*-value < 0.05 were reported as significantly increased or decreased.

Genome sequencing, assembly and variant calling

We used the Illumina HiSeq 2000 platform with 96-fold multiplexing, read lengths of 100 or 150 bp, insert sizes of 200 bp, and mean depth of 125 reads. As previously described (4), we used Velvet (15) to assemble reads into contigs *de novo* for each genome. We used Stampy (16) with no BWA premapping and an expected substitution rate of 0.01 to map the reads of each isolate against MRSA252 (17), USA300 (18) and host-specific draft genomes assembled by Velvet. We used xBASE (19) to annotate the draft genome assemblies. We used SAMtools (20) and Picard (http://picard.sourceforge.net) to call single nucleotide polymorphisms (SNPs) from mapping, which we filtered using published criteria (4). We additionally used Cortex (21) to detect SNPs and indels.

Transcriptome analysis by RNA deep sequencing and determination of transcription initiation sites

RNA was isolated as previously described (22) or bacterial mRNA from overnight cultures was extracted using the RNeasy Protect Bacteria Kit (Qiagen) according to the manufacturer instructions (protocol 4). DNase I (DNAfree kit, Ambion) was used to remove remaining DNA. The concentration of the RNA was determined by spectrophotometry on a Nanodrop 1000 (Peqlab) or via fluorometry using the Qubit Fluorometer RNA BR Kit (Invitrogen). Quality and quantity of the RNA was examined using either 1.8% agarose gel containing formamide or by analysis on Tapestation (Agilent Technologies).

When required enrichment of mRNA was done using the Universal Ribodepletion Kit (Epicentre) followed by Next Ultra Directional Library Preparation Kit for Illumina (NEB). For the depletion of processed transcripts, equal amounts of RNA were incubated with Terminator 5'-phosphate-dependent exonuclease (TEX) (Epicentre #TER51020) as previously described (23). The Library preparation and sequencing was done by the High Throughput Genomics facility, Wellcome Trust Centre for Human Genomics (Oxford, UK) or by Vertis Biotechnology AG, Germany

(http://www.vertis-biotech.com/) as described previously for eukaryotic microRNAs (24) but omitting the RNA size-fractionation step prior to cDNA synthesis. For Terminator 5' exonuclease treatment and enrichment of transcription initiation sites RNA samples were poly(A)-tailed using poly(A) polymerase and 5'-triphosphates were removed by treatment with tobacco acid pyrophosphatase (TAP). RNA adapter was ligated to the 5'-phosphate of the RNA. First-strand cDNA was generated using an oligo(dT)-primer and M-MLV reverse transcriptase. Using a high fidelity DNA polymerase cDNA was amplified to 20-30 ng/µl by PCR.

The cDNA was sequenced on HiSeq™ 2000 or 2500 (Illumina) yielding 100 bp paired end reads. At least 28 Million, 100 bp long paired-end reads were adapter removed and trimmed to 70 bp using trimmomatic (25) and only reads exceeding a mean base quality 5 within all sliding windows of 5bp were mapped to the *S. aureus* USA300 FPR3757 genome (NCBI accession NC_007793.1). Read mapping was conducted using Bowtie2 (26) and only paired and concordant alignments were considered further, yielding at least 12 million uniquely mapped read pairs per replicate. To quantify per-gene read counts, htseq (27) was used counting only reads with an alignment quality of greater than 10 in mode 'union'. A total of 2693 coding and non-coding transcripts were identified for further analysis.

Differential transcript abundance analysis was performed using the DESeq2 package v.1.5.9 (13) in R. We fitted two models in which the number reads mapping to gene *i* in sample *j* was modelled using a negative binomial distribution with mean

$$E\left(K_{ij}\right) = s_j q_{ij}$$

and dispersion factor α_i, where s_j is a sample-specific size factor accounting for different sequencing depth among samples and q_{ij} is a log-linear predictor of gene expression as a function of the genetic background of sample *j* (B_j = [USA300,P,S]) and the *rsp* status (R_j = [*rsp*$^+$, *rsp*$^-$]). In the additive model,

$$\log_2 q_{ij} = b_i + g_{i,B_j} + d_{i,R_j},$$

and in the interaction model,

$$\log_2 q_{ij} = b_i + g_{i,B_j} + d_{i,R_j} + h_{i,B_j,R_j}.$$

Here β_i is the intercept, $\gamma_{i,B}$ is the main effect of genetic background *B*, $\delta_{i,R}$ is the main effect of *rsp* status *R* and $\eta_{i,B,R}$ is the non-additive component of the interaction between genetic background and *rsp* status. We used the approximate Bayesian procedure in DESeq2 to obtain maximum *a posteriori* (MAP) estimates of the model parameters. We tested for significant effects using the Bayesian Wald test in DESeq2, a screening procedure motivated by Bayesian decision theory that produces *p*-values with frequentist properties (28). Transcripts with low counts were filtered out to improve power (29) and the Benjamini-Hochberg adjustment of the *p*-values was employed to obtain an expected false discovery rate (FDR) of 10% (14).

Gene set enrichment analysis

For the gene set enrichment analysis (GSEA), we modelled the number of mutations of a particular type (synonymous, replacement or truncating) as Poisson distributed with expectation equal to the length of the gene multiplied by a coefficient. Under the null hypothesis, this coefficient was estimated for all genes and under the alternative hypothesis, two separate coefficients were estimated: one for the genes in a gene set and another for the rest. GSEA categories were obtained from Biocyc annotations for MRSA252 (30), with lift over to the USA300 gene set using Ortholuge (31).

Transcriptional start site mapping

For TEX-treated single end reads, the Illumina reads in FASTQ format were trimmed with a cut-off phred score of 20 by the program fastq_quality_trimmer from FASTX toolkit version 0.0.13 (http://hannonlab.cshl.edu/fastx_toolkit/). The following steps were performed using subcommand

"create", "align" and "coverage" of the tool READemption (32) version 0.1.6. The poly(A)-tail sequences were removed and a size filtering step was applied in which sequences shorter than 12 nt were eliminated. The collections of remaining reads were mapped to the reference genome sequences using segemehl (33). Coverage plots in wiggle format representing the number of aligned reads per nucleotide were generated based on the aligned reads and visualized in the Integrated Genome Browser (34). Each graph was normalized to the total number of reads that could be aligned from the respective library. To restore the original data range and prevent rounding of small error to zero by genome browsers, each graph was then multiplied by the minimum number of mapped reads calculated over all libraries.

Quantitative Real time PCR (qRTPCR)

The DNase I treated RNA was converted into cDNA by using either the QuantiTect® Reverse Transcription Kit (Qiagen) or SuperScriptII (Invitrogen) according to the manufacturer's recommendations. Real time PCR was performed on a StepOne® Plus Real Time PCR system (Applied Biosystems) using SYBR® Green PCR master mix. Primers used are listed in SI Appendix, Table S3.

Peroxide stimulation assay

Bacteria were grown overnight in TSB at 37°C with shaking at 200 rpm in air. For stationary phase samples, the overnight cultures were washed with PBS and resuspended in fresh TSB. For logarithmic phase, overnight cultures were diluted in fresh TSB ($OD_{600=}$ 0.1) and incubated in air at 37°C with shaking (200 rpm) until mid-logarithmic phase ($OD_{600=}$ 0.6). Bacterial suspensions were transferred to microfuge tubes, treated with hydrogen peroxide at a final concentration of 5 mM and incubated at 37°C for 10 minutes with shaking (200 rpm). Bacteria were harvested by centrifugation at 14,000 rpm for 30 seconds and pellets were flash frozen in liquid nitrogen. The pellets were then used for RNA extraction. Alternatively, after treatment at mid-logarithmic phase,

the bacteria were allowed to grow until 8 hours post inoculation. The supernatants were collected by centrifugation and sterile filtration and were tested for cytotoxic potential.

Secreted proteome analysis

Sample preparation for extracellular secreted proteome analysis

Bacterial strains were grown in overnight at 37°C, 180 rpm shaking in both Tryptone-soy broth (TSB, Oxoid) and in α-MEM (Life Technologies), in parallel. Bacteria were pelleted from cultures by centrifugation (10000 x g, 20 min, 4°C) and supernatants aspirated. Proteins were precipitated from 200 µL of supernatant with methanol/chloroform. Protein pellets were re-solubilized in 6 M urea solution in 0.1 M TRIS (pH 7.8). After 20 min resolubilization, dithiothreitol (DTT) (final concentration of 20 mM in 0.1 M Tris) and iodoacetamide were added (final concentration of 40 mM) for cysteine alkylation for further 20 min incubation at room temperature. The DTT treatment was repeated with 40 mM DTT to consume remaining alkylation reagent. Samples were diluted with water to a final concentration of 1 M urea and 0.2 µg trypsin was added for overnight digestion. Salts were removed from the sample using a C18 Sep-Pak column (Light, Waters), washed with buffer A (2% Acetonitrile, 0.1% formic acid in water) and eluted with buffer B (98% Acetonitrile, 0.1% formic acid in water). Purified peptides were dried using a vacuum manifold before re-suspension in Buffer A.

Liquid Chromatography Tandem Mass Spectrometry

Peptides were separated on an Dionex Ultimate 3000 UPLC system (Thermo Scientific) supplemented with a 50 cm x 75 µm Acclaim PepMap RSLC column, 2 µm particle size using a linear gradient from 2-35% buffer B (5% DMSO, 0.1% formic acid in acetonitrile) into buffer A (5% DMSO, 0.1 % formic acid in water) at a flow rate of 250 nl/min (at approx. 600 bar) for 60 min. Peptides were introduced to a TripleTOF 5600 mass spectrometer (AB Sciex) by electrospray ionization. CID fragmentation using ramped collision energy was induced on the 30 most abundant ions per full MS

scan with a total cycle time of 3.3 s. All fragmented precursor ions were actively excluded from repeated selection for 15 s.

Mass Spectrometry data analysis and interpretation

Data (wiff-files) were converted to MASCOT generic files using ProteinPilot (35). Sequence interpretation of MS/MS spectra were performed with PEAKS (36) using bacterial-backbone specific databases, together with (in all cases) all 74,380 UniProt entries for the soybean plant (*Glycine max,* NCBI taxon id 3847). This was included to estimate soybean protein detection in bacterially-conditioned tryptone soy broth. The probability score threshold was defined by decoy database searches implemented in the regarding search engines at a general false discovery rate of 1%. For USA300 strains, the protein database used contained all 2604 annotated proteins of the USA300 strain of *Staphylococcus aureus* (NCBI accession NC_007793.1). For isolates P and S, we identified homologues of the 2604 protein in USA300 by comparison of USA300 proteins with Velvet assemblies of whole genome sequencing of strains from P and S using the NCBI Blast+ Suite 2.2.6 tblastn program. The single best hit with an e-value < 10^{-5} and a similar amino acid: query length ratio of > 0.7 was retained and considered to be a homologue of the USA300 predicted protein used as a query. Overall 2,411 homologues were found in either P or S genomes. The protein databases used are attached as Supp. Data S5. Abundances were computed from the top 3 peptides shared by all gene homologs in NC_007793.1, and genomes P and S. Although not strictly count data, the decoupling of mean and variance in the negative binomial distribution assumed by DESeq2 enabled us to model differential secreted protein abundance in an identical manner to the transcript abundances by discretizing the abundance. This assisted direct comparison between the results of the transcriptomic and proteomic analyses.

Comparison of secreted proteins in Tryptone Soy Broth and α–MEM

We analyzed the supernatants of stationary phase cultures of various bacterial backgrounds grown in both Tryptone Soy Broth (TSB) and αMEM (Life Technologies), a protein-free medium, using mass

spectrometry (described above). The means of two biological replicates were determined. Proteins not detected were considered to have an abundance of zero. To understand differences between secretion in TSB and αMEM, Spearman's rank correlation coefficient was computed between different isolates and conditions, and visualized using the corrplot package in R 3.1.11 for Linux.

Hemolysis assays

Bacteria were grown overnight in TSB at 37°C. The culture was diluted 1:100 in fresh TSB medium and 10 µL was spotted on Columbia agar supplemented with 5% defibrinated sheep blood and incubated overnight at 37°C. The resulting bacterial colonies were photographed by using an Olympus SZ261 Binocular at 5x magnification. The magnitude of hemolysis was examined by calculating the diameter of hemolysis using ImageJ. The diameter of hemolysis for each set was calculated by using the following formula.

Zone of hemolysis (mm) = Diameter of erythrocyte lysis zone – Diameter of colony

The measurements were plotted as bar graphs showing the mean zone of hemolysis and standard deviation for comparison between wild type, mutant and complemented strains, each group made in biological triplicates. Statistical significance was calculated by using one way-ANOVA and Tukey's post hoc analysis.

Cell death assays

HeLa cells were grown on 12 well plates in RPMI1640 medium (Invitrogen) supplemented with 10% FCS (PAA), 1 mM sodium pyruvate (Invitrogen). *S. aureus* cultures were grown overnight in TSB and the cultures were diluted to an OD_{600} of 0.4 in 10 ml fresh TSB medium and incubated for 1 h at 37°C (200 rpm). Bacteria were washed, resuspended in tissue culture medium and used for infection at a MOI of 10. Extracellular bacteria were removed by lysostaphin/gentamicin treatment 1-hour post infection and were further incubated with only gentamicin.

After infection, the supernatant (which may contain dead cells) was collected and residual cells detached by treatment with Trypsin/EDTA solution (Life Technologies) for 3 minutes. Trypsinization was stopped by re-addition of the supernatant. After this, all samples were collected by centrifugation at 500 x g for 5 minutes. The cells were resuspended in FACS labelling solution (10 mM HEPES pH 7.4, 140 mM NaCl, 5 mM $CaCl_2$, 1% [v/v] propidium iodide). The reaction was incubated in the dark for 10 minutes at room temperature. After the incubation, the cells were diluted 1:5 with incubation buffer and analyzed immediately using a Accuri C6 flow cytometer using 488 nm and a band pass filter (610-630 nm, FL3) for fluorescence detection. A gate was defined in forward scatter and side scatter, which anticipated alteration of host cell morphology during the course of infection and the resulting pathogen-induced cell death. The mean percentages of propidium iodide stained cells were plotted and statistical calculation was performed using one way-ANOVA and Tukey's post hoc analysis.

Phagosomal escape assay

Phagosomal escape was examined as described previously with minor modifications (37, 38). Briefly, HeLa cells expressing YFP-CWT fusion (37, 39) were grown dark 24 well plates (ibidi µ-clear) in RPMI1640 medium (Invitrogen) supplemented with 10% FCS, 1 mM sodium pyruvate. *S. aureus* cultures were grown overnight in TSB (37 °C, 200 rpm) and the cultures were diluted to an OD_{600} of 0.4 in 10 ml TSB medium and incubated for 1h at 37°C. Bacteria were harvested by centrifugation, labelled with 50 µg/ml TRITC (mixed isomers; MoBiTec) for 30 min at 37°C and used for infecting the HeLa cells at an MOI of 10. Extracellular bacteria were removed by Lysostaphin (AMBI, Lawrence, NY, USA; final concentration 20 µg/ml) and Gentamicin (Invitrogen; final concentration 100 µg/ml) treatment 1 hour post infection and were further incubated an additional 2 hours. The cells were washed with 1x PBS containing Ca^{2+} and Mg^{2+} and subsequently fixed with 4% paraformaldehyde. The samples were observed on an automated Operetta Fluorescence Microscope (Perkin Elmer).

Phagosomal escape was examined by investigating co-localization of YFP and TRITC signals with the embedded Harmony software (Perkin Elmer). The wild type strain USA300 JE2 and an *agrA* mutant (NE1532) served as the positive and negative controls, respectively. The mean escape scores were plotted and statistical significance was calculated by Student's t-test with wild type as the reference.

Intracellular replication assay

S. aureus strain 6850 and its *rsp* mutant were transformed with pmRFPmars encoding a red-fluorescent protein (3) using standard techniques. HeLa cells were infected for 60 min with red fluorescent bacteria at an MOI of 10 and extracellular bacteria were removed by treatment with Lysostaphin and Gentamicin as published (38). After 90 minutes and 180 minutes post infection, host cells were trypsinized, transferred to phenol-red free RPMI1640 medium (Invitrogen) and immediately analyzed on a FACSAriaIII (BD) using the 561 nm laser. Forward and side scatter gating was applied to intact epithelial cells and fluorescence intensity within the gate was measured. Red-fluorescent bacteria and uninfected host cells served as experimental controls. The intensity of red fluorescence (arbitrary fluorescent units, AFU) corresponds to the amount of intracellular bacteria.

***S. aureus* neutrophil cytotoxicity**

Primary human polymorphonuclear leucocytes (PMNs) were isolated as described previously (40). The neutrophils were harvested by centrifugation at 1,000 rpm for 5 minutes and resuspended in 1x Hank's Balanced Salt Solution (HBSS). Neutrophil killing by intracellular *S. aureus* was examined as previously described (41). At 10, 30, 60, 120 and 240 minutes post infection, neutrophils were collected by centrifugation and supernatants were used to measure the release of neutrophil lactate dehydrogenase (LDH) by the Cytotoxicity Detection Kit PLUS (Roche) according to manufacturer's instructions. To examine killing of ingested *S. aureus,* neutrophils were lysed with sterile water at pH 11.0 for 5 minutes, vortexed, serially diluted to 10^{-1}, 10^{-3}, 10^{-5} and plated on TSA containing appropriate antibiotics. The plates were incubated at 37°C overnight and bacterial colonies were

counted. For assessment of the toxicity of *S. aureus* culture supernatants primary human neutrophils were treated with sterile-filtered bacterial supernatants from either peroxide stimulated cultures or overnight cultures, at a final concentration of 1% (v/v) in infection medium. The cells were then incubated at 37°C by tumbling on a rotator for 2 and 4 hours. Vehicle controls used unconditioned bacterial growth medium. At each time point, the neutrophils were centrifuged at 500 x g for 5 minutes and LDH release was determined (see above).

Murine infection models

Pneumonia model

Female BALB/c mice aged 6 weeks were purchased from Charles River (Sulzfeld, Germany) and were kept in individually ventilated cages on a normal diet in six groups of 5. At 8 weeks, groups of 10 mice were infected intranasally with a bacterial suspension, prepared as described above. The instilled lethal doses in a 20 µl inoculum were 2 x 10^8 cfus for USA300 LAC* and 0.7 x 10^8 cfus *for S. aureus* 6850, respectively. Weight loss and survival was monitored at an interval of 24 hours for 3 days. At each time point deceased mice were removed from the cages and transferred for disinfection and disposal. At the end of 3 days, the surviving mice were sacrificed by CO_2 inhalation. The survival was analyzed by Kaplan-Meier estimate and statistical significance was calculated by Mantel-Cox Log-rank test, using GraphPad Prism 6 for Mac OSX.

Intravenous model

Female BALB/c mice aged 6 weeks were obtained from Taconic Biosciences Inc. (Denmark) and housed in individually filtered cages on a normal diet in four groups of 6. At 8 weeks, mice were inoculated i.v. in the lateral tail vein with 0.1 mL bacterial suspensions in PBS at a dose of 5x10^6 cfu per mouse. Weight and clinical score/survival was monitored with a scoring system based on published work (42, 43) and which is included in SI Appendix, Table S4. 3 hours or 3 days post infection, mice were sacrificed (terminal anesthesia with Isoflurane followed by dislocation of the

neck), blood, livers, spleens and right kidney taken and viable *S. aureus* per gram of tissue/ml of blood were enumerated by spreading serial diluted aliquots of homogenized tissue (GentleMACS, M-tubes, Miltenyi Biotec, Bisley, UK) for colony formation using an Autoplate machine (Quadrachem, UK) on horse blood agar (HBA) (Oxoid). Plates were incubated for 24 hours at 37°C in air, and colonies were counted using an automated counter (QCount, Quadrachem, UK). Mann-Whitney tests were used to compare animal weights and severity scores following infection. Kaplan-Meier survival curves were constructed based on time taken to reach a humane endpoint. The association between *rsp* genotype and survival was assessed using a log-rank test. Analyses described in this section used GraphPad Prism 6 for Windows.

Renal histopathology

48 hours post intravenous infection, kidneys were harvested and stored in 4 % paraformaldehyde (PFA) (Sigma). Following embedding in wax, three 5µM sections were taken through the long (sagittal) axis of each kidney at approximately 15%, 35% and 50% renal thickness and stained with haematoxylin and eosin staining in the Oxford Centre for Histological Research (OCHRE), John Radcliffe Hospital, Oxford. Images were scanned using a Hamamatsu C600 Nanozoomer slide scanner and visualised with ImageScope (Aperio) software. Abscesses were defined as areas of focal neutrophil infiltration.

Supplementary Figure Legends

Figure S1: Mapping of transposon insertion sites (TIS) by deep sequencing (TnSeq) of a *S. aureus* mutant library.

A, On average, 8.84 TIS were identified per 1 kb bin along the *S. aureus* 6850 genome. **B,** The impact of *rsp* mutation on growth rates was analyzed. There is no evidence the growth rates differed (growth rate of wild type relative to mutant was 1.07 (95% CI 0.79-1.47)). **C**, Intracellular replication of *S. aureus* expressing mRFP was measured by flow cytometry. *S. aureus* 6850 wild type demonstrated significant intracellular replication, and *rsp* mutants showed a similar rate of replication within HeLa cells. Means (±SD) of arbitrary fluorescent units (AFUs) are plotted for time points 90 and 180 minutes post infection (n=3). **D,** *rsp* gene disruption does not influence gentamicin susceptibility. MIC was determined by using antibiotic sensitivity test strips in both backgrounds, 6850 and USA300 LAC*. Mutants in *rsp* were compared to the wild type (WT) and *rsp* complemented mutants (*rsp* comp). In all strains the MIC was observed at 0.5 µg/ml (arrows).

Figure S2: Rsp is a regulator of cytotoxicity, but influences neither host cell invasion nor phagosomal escape.

Rsp neither influences neither host cell invasion nor phagosomal escape. A, Cell invasion is not significantly affected upon *rsp* deletion. WT, mutant and complemented mutant (Comp) demonstrated similar invasion rates into HeLa as evidenced with gentamicin protection assays. B, Phagosomal escape did not differ significantly between the *rsp* mutant and the wild type (WT). By contrast, the capacity of the *agr*A mutant to escape from the phagosome was strongly reduced. Error bars reflect standard deviations.

Figure S3: Influence of *rsp* gene disruption on infection lethality in mice.

A, Lethality in a pulmonary challenge model with the *S. aureus* 6850 strain, or its *rsp* mutant, with and without complementation. The comparison shown is for a log-rank test comparing wild type with mutant 6850 strains. **B**, Illness score of USA300 rsp^+ and rsp^- injected mice over three days. Scores were determined twice daily (see SI Materials and Methods) and animals with a score higher than seven were sacrificed and considered "endpoint" (dotted line). Animals which had been sacrificed were arbitrarily given illness scores of 15. Comparison of (**C**) severity scores between the two groups USA300 rsp^+ and rsp^- and (**D**) weight loss after infection in percentage from day 0 (day of challenge) weight representing 100 %. The red line shows the average weight of USA300 rsp^+ challenged mice, the black line the average of USA300 rsp^- challenged mice. At day 3, a number of animals had reached the humane endpoint, and the data shown is derived only from survivors; at day 2, all animals were weighed.

Figure S4: *rsp* mutants and wild-types form renal abscesses.

A, 48 hours after intravenous infection, kidneys were harvested and analyzed histologically. Numbers of abscesses were identified in 9 kidneys per group (54 in total). Areas showing neutrophil enrichment in a hematoxylin and eosin stain were counted as abscess. The results shown here are for USA300 JE2 (rsp^+) and USA300 NE1304 (rsp^-). **B,** A representative histological image of a kidney infected with USA300 JE2 (*rsp+*) shows formation of 3 abscesses. **C,** A 14x magnification of one of the USA300 JE2 (rsp^+) abscesses. **D,** USA300 NE1304 (rsp^-) infected kidney, showing that early abscess formation occurs independent of *rsp*. **E,** enlargement of the abscess indicates similar abscess architectures in the mutant infected kidneys.

Figure S5: By gene significance estimates from RNA-seq.

Effect of *rsp* mutation on gene transcription, determined by DESeq2 fitting of three separate models, one for each of three *S. aureus* backgrounds (Patient S, Patient P and USA300), estimating effects per-gene from RNA-seq data in stationary phase. Shown is $-\log_{10}(q)$, where q is the adjusted significance estimate for the effect of the *rsp* mutant across each genome. Similar patterns of significance are evident.

Figure S6: *rsp* is a regulator of virulence-associated genes.

Transcript abundance was determined by real-time PCR in wild type (WT), *rsp* mutant (mutant) and complemented mutant (Comp) from exponential **(A,C)** or stationary phase cultures (**B,D**) of *S. aureus* 6850 or USA300 LAC*. **A,** The transcription of the global virulence regulators *agr*A and *sig*B (syn. *rpo*F) encoding the response regulator of the accessory gene regulator (*agr*) quorum-sensing system and the alternative sigma factor B, are independent of *rsp* in both strain backgrounds. The leukocidin subunit *luk*B, chemotaxis inhibitor *chs*, the staphopain A protease *scp*A as well as the ncRNA *SSR*42 are *rsp*-dependently expressed. Due to episomal location of the complementation construct, transcript levels exceed wild type levels in complemented mutants (Comp.). Statistical analysis for each target was performed by one-way ANOVA and Tukey's post-hoc analysis; *p<0.05, **p < 0.01, ***p< 0.001.

Figure S7: Detection of proteins in supernatants of bacterial strains. We investigated the secreted proteome of three strains (USA300 JE2, and the patient P and S nasal isolates) and their corresponding *rsp* mutants by analyzing supernatants of a range of stationary phase bacterial cultures grown in either Tryptone Soy Broth (TSB) or αMEM, a protein-free medium. In total, 651 of the 2,604 proteins sought were identified in the supernatant in any sample. **A** Correlation between

protein abundances under different conditions. The figure illustrates the Spearman rank coefficient ρ for the detected abundances of 651 proteins which were detected under the conditions examined. Proteins not detected were considered to have zero abundance. Protein abundances between individual strains are strongly correlated. Correlations are stronger with proteins detected in TSB than in αMEM. This reflects (**B)** The sensitivity of detection by of the 651 detectable proteins in pairs of supernatants. Thus, 1 reflects detection of all 651 proteins. Consistently fewer proteins were detected in TSB (about 50%) than in αMEM. Based on the higher sensitivity of detection in αMEM, the main manuscript describes results obtained using αMEM.

Figure S8: *rsp* effects are induced by hydrogen peroxide.

A, The known peroxide-inducible transcription of *dps* is partially dependent on *rsp.* Wild type *S. aureus* (WT), its isogenic *rsp* mutant, and in the complemented mutant (Comp), *dps* transcript levels are significantly increased in the peroxide-treated (white bars) samples relative to untreated controls (dark bars). **B,** *rsp*-dependent peroxide inducibility was also observed in *S. aureus* 6850, thereby indicating a strain independent regulatory mechanism. Statistical analysis was performed by pair-wise t-test. *$p < 0.05$, **$p<0.01$, ***$p<0.001$.

Supplementary Data

Supplementary Data S1: Detailed list of TnSeq screening results of *S. aureus* Himar1 transposon mutant library in epithelial cells (related to Table 1).

Supplementary Data S2: RNA-seq results for stationary phase cultures of USA300 JE2, as well as blood stream isolates from patients P and S.

Supplementary Data S3: Survey of *rsp*-dependent transcriptional changes of USA300 within exponential growth phase.

Supplementary Data S4: Master table of proteomics analysis for stationary phase cultures supernatants of USA300 JE2, as well as blood stream isolates from patients P and S.

Supplementary Data S5: Protein databases used for proteomic analyses of backgrounds P and S. These are attached in excel format.

Supplementary References

1. **Bae T & Schneewind O (2006) Allelic replacement in *Staphylococcus aureus* with inducible counter-selection. *Plasmid* 55(1):58-63.**
2. **Lofblom J, Kronqvist N, Uhlen M, Stahl S, & Wernerus H (2007) Optimization of electroporation-mediated transformation: *Staphylococcus carnosus* as model organism. *J Appl Microbiol* 102(3):736-747.**
3. **Paprotka K, Giese B, & Fraunholz MJ (2010) Codon-improved fluorescent proteins in investigation of *Staphylococcus aureus* host pathogen interactions. *Journal of microbiological methods* 83(1):82-86.**
4. **Young BC, *et al.* (2012) Evolutionary dynamics of Staphylococcus aureus during progression from carriage to disease. *Proc Natl Acad Sci U S A* 109(12):4550-4555.**
5. **Rice P, Longden I, & Bleasby A (2000) EMBOSS: the European Molecular Biology Open Software Suite. *Trends in genetics : TIG* 16(6):276-277.**
6. **Pearson WR, Wood T, Zhang Z, & Miller W (1997) Comparison of DNA sequences with protein sequences. *Genomics* 46(1):24-36.**
7. **Finn RD, *et al.* (2014) Pfam: the protein families database. *Nucleic acids research* 42(Database issue):D222-230.**
8. **Lei MG, Cue D, Roux CM, Dunman PM, & Lee CY (2011) Rsp inhibits attachment and biofilm formation by repressing fnbA in Staphylococcus aureus MW2. *Journal of bacteriology* 193(19):5231-5241.**
9. **Li M, *et al.* (2009) *Staphylococcus aureus* mutant screen reveals interaction of the human antimicrobial peptide dermcidin with membrane phospholipids. *Antimicrobial agents and chemotherapy* 53(10):4200-4210.**
10. **Gilbert JA, *et al.* (2010) The taxonomic and functional diversity of microbes at a temperate coastal site: a 'multi-omic' study of seasonal and diel temporal variation. *PloS one* 5(11):e15545.**
11. **Martin JA & Wang Z (2011) Next-generation transcriptome assembly. *Nature reviews. Genetics* 12(10):671-682.**
12. **Langmead B & Salzberg SL (2012) Fast gapped-read alignment with Bowtie 2. *Nat Methods* 9(4):357-359.**
13. **Love MI, Huber W, & Anders S (2014) Moderated estimation of fold change and dispersion for RNA-seq data with DESeq2. *Genome biology* 15(12):550.**
14. **Benjamini Y & Hochberg Y (1995) Controlling the False Discovery Rate - a Practical and Powerful Approach to Multiple Testing. *J Roy Stat Soc B Met* 57(1):289-300.**
15. **Zerbino DR & Birney E (2008) Velvet: algorithms for de novo short read assembly using de Bruijn graphs. *Genome research* 18(5):821-829.**
16. **Lunter G & Goodson M (2011) Stampy: a statistical algorithm for sensitive and fast mapping of Illumina sequence reads. *Genome research* 21(6):936-939.**
17. **Holden MT, *et al.* (2004) Complete genomes of two clinical Staphylococcus aureus strains: evidence for the rapid evolution of virulence and drug resistance. *Proc Natl Acad Sci U S A* 101(26):9786-9791.**
18. **Diep BA, *et al.* (2006) Complete genome sequence of USA300, an epidemic clone of community-acquired meticillin-resistant *Staphylococcus aureus*. *Lancet* 367(9512):731-739.**
19. **Chaudhuri RR, *et al.* (2008) xBASE2: a comprehensive resource for comparative bacterial genomics. *Nucleic acids research* 36(Database issue):D543-546.**

20. **Li H, *et al.* (2009) The Sequence Alignment/Map format and SAMtools. *Bioinformatics* 25(16):2078-2079.**
21. **Iqbal Z, Caccamo M, Turner I, Flicek P, & McVean G (2012) De novo assembly and genotyping of variants using colored de Bruijn graphs. *Nature genetics* 44(2):226-232.**
22. **Lasa I, *et al.* (2011) Genome-wide antisense transcription drives mRNA processing in bacteria. *Proc Natl Acad Sci U S A* 108(50):20172-20177.**
23. **Sharma CM, *et al.* (2010) The primary transcriptome of the major human pathogen *Helicobacter pylori*. *Nature* 464(7286):250-255.**
24. **Berezikov E, *et al.* (2006) Diversity of microRNAs in human and chimpanzee brain. *Nature genetics* 38(12):1375-1377.**
25. **Bolger AM, Lohse M, & Usadel B (2014) Trimmomatic: a flexible trimmer for Illumina sequence data. *Bioinformatics* 30(15):2114-2120.**
26. **Langmead B, Trapnell C, Pop M, & Salzberg SL (2009) Ultrafast and memory-efficient alignment of short DNA sequences to the human genome. *Genome biology* 10(3):R25.**
27. **Anders S, Pyl PT, & Huber W (2015) HTSeq--a Python framework to work with high-throughput sequencing data. *Bioinformatics* 31(2):166-169.**
28. **Rice K (2010) A Decision-Theoretic Formulation of Fisher's Approach to Testing. *The American Statistician* 64(4):345-349.**
29. **Bourgon R, Gentleman R, & Huber W (2010) Independent filtering increases detection power for high-throughput experiments. *Proc Natl Acad Sci U S A* 107(21):9546-9551.**
30. **Caspi R, *et al.* (2014) The MetaCyc database of metabolic pathways and enzymes and the BioCyc collection of Pathway/Genome Databases. *Nucleic Acids Res* 42(Database issue):D459-471.**
31. **Whiteside MD, Winsor GL, Laird MR, & Brinkman FS (2013) OrthologeDB: a bacterial and archaeal orthology resource for improved comparative genomic analysis. *Nucleic Acids Res* 41(Database issue):D366-376.**
32. **Forstner KU, Vogel J, & Sharma CM (2014) READemption-a tool for the computational analysis of deep-sequencing-based transcriptome data. *Bioinformatics* 30(23):3421-3423.**
33. **Hoffmann S, *et al.* (2009) Fast mapping of short sequences with mismatches, insertions and deletions using index structures. *PLoS computational biology* 5(9):e1000502.**
34. **Nicol JW, Helt GA, Blanchard SG, Jr., Raja A, & Loraine AE (2009) The Integrated Genome Browser: free software for distribution and exploration of genome-scale datasets. *Bioinformatics* 25(20):2730-2731.**
35. **Shilov IV, *et al.* (2007) The Paragon Algorithm, a next generation search engine that uses sequence temperature values and feature probabilities to identify peptides from tandem mass spectra. *Molecular & cellular proteomics : MCP* 6(9):1638-1655.**
36. **Zhang J, *et al.* (2012) PEAKS DB: de novo sequencing assisted database search for sensitive and accurate peptide identification. *Molecular & cellular proteomics : MCP* 11(4):M111 010587.**
37. **Grosz M, *et al.* (2014) Cytoplasmic replication of *Staphylococcus aureus* upon phagosomal escape triggered by phenol-soluble modulin alpha. *Cell Microbiol* 16(4):451-465.**

38. **Giese B, *et al.* (2011) Expression of delta-toxin by *Staphylococcus aureus* mediates escape from phago-endosomes of human epithelial and endothelial cells in the presence of beta-toxin. *Cell Microbiol* 13(2):316-329.**
39. **Gründling A & Schneewind O (2007) Synthesis of glycerol phosphate lipoteichoic acid in *Staphylococcus aureus*. *Proc Natl Acad Sci U S A* 104(20):8478-8483.**
40. **Hattar K, *et al.* (2001) Subthreshold concentrations of anti-proteinase 3 antibodies (c-ANCA) specifically prime human neutrophils for fMLP-induced leukotriene synthesis and chemotaxis. *Journal of leukocyte biology* 69(1):89-97.**
41. **Pang YY, *et al.* (2010) agr-Dependent interactions of *Staphylococcus aureus* USA300 with human polymorphonuclear neutrophils. *Journal of innate immunity* 2(6):546-559.**
42. **Langford DJ, *et al.* (2010) Coding of facial expressions of pain in the laboratory mouse. *Nature methods* 7(6):447-449.**
43. **Bremell T, Lange S, Yacoub A, Ryden C, & Tarkowski A (1991) Experimental *Staphylococcus aureus* arthritis in mice. *Infect Immun* 59(8):2615-2623.**

Figure S1

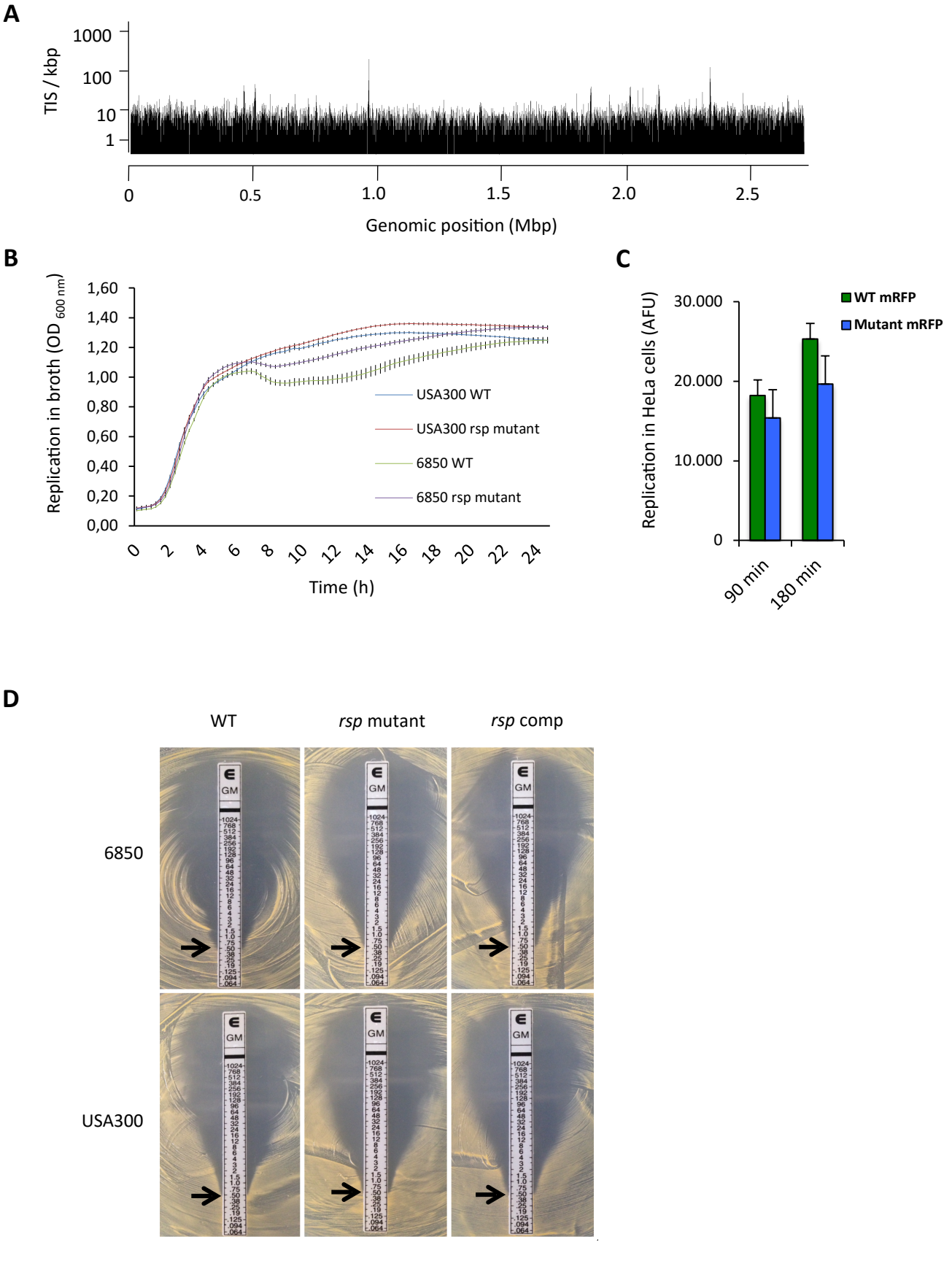
A
TIS / kbp
1000
100
10
1
0
0.5
1.0
1.5
2.0
2.5
Genomic position (Mbp)
B
Replication in broth (OD 600 nm)
1,60
1,40
1,20
1,00
0,80
0,60
0,40
0,20
0,00
0
2
4
6
8
10
12
14
16
18
20
22
24
Time (h)
USA300 WT
USA300 rsp mutant
6850 WT
6850 rsp mutant
C
Replication in HeLa cells (AFU)
30.000
20.000
10.000
0
90 min
180 min
WT mRFP
Mutant mRFP
D
WT
rsp mutant
rsp comp
6850
USA300
GM

Figure S2

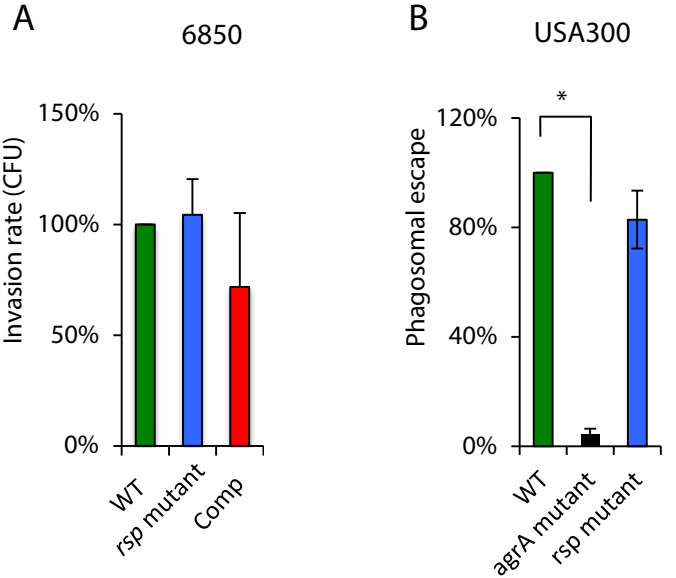
A
6850
Invasion rate (CFU)
150%
100%
50%
0%
WT
rsp mutant
Comp
B
USA300
Phagosomal escape
120%
80%
40%
0%
*
WT
agrA mutant
rsp mutant

Figure S3

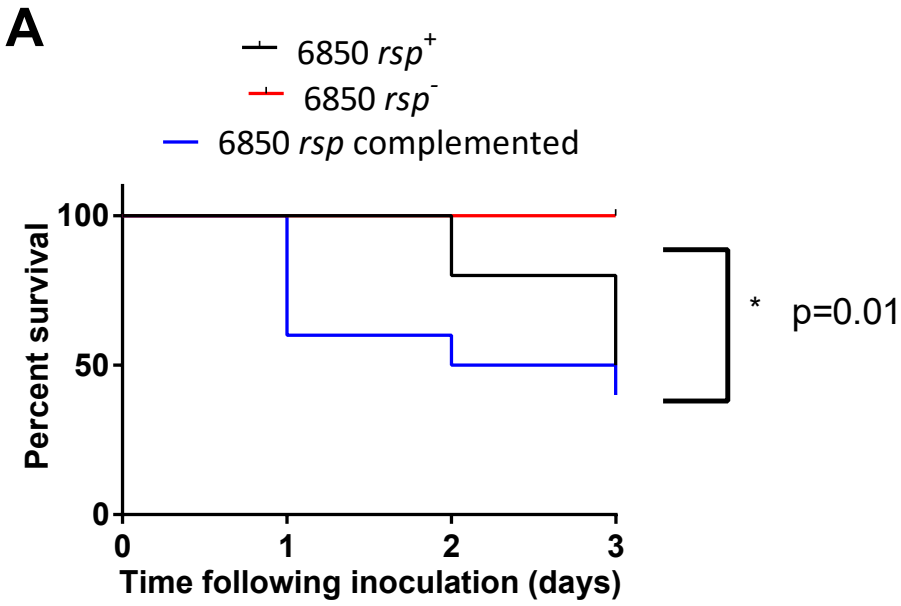
A
6850 rsp+
6850 rsp-
6850 rsp complemented
Percent survival
100
50
0
0
1
2
3
Time following inoculation (days)
*
p=0.01

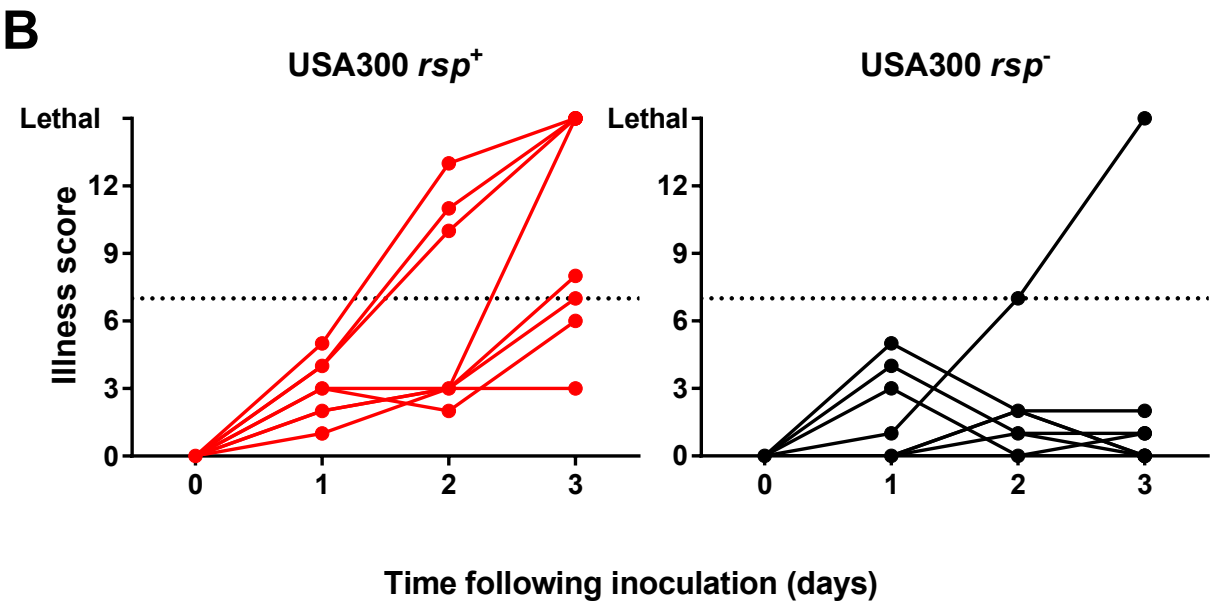
B
USA300 rsp+
USA300 rsp-
Lethal
Lethal
Illness score
12
9
6
3
0
0
1
2
3
Time following inoculation (days)

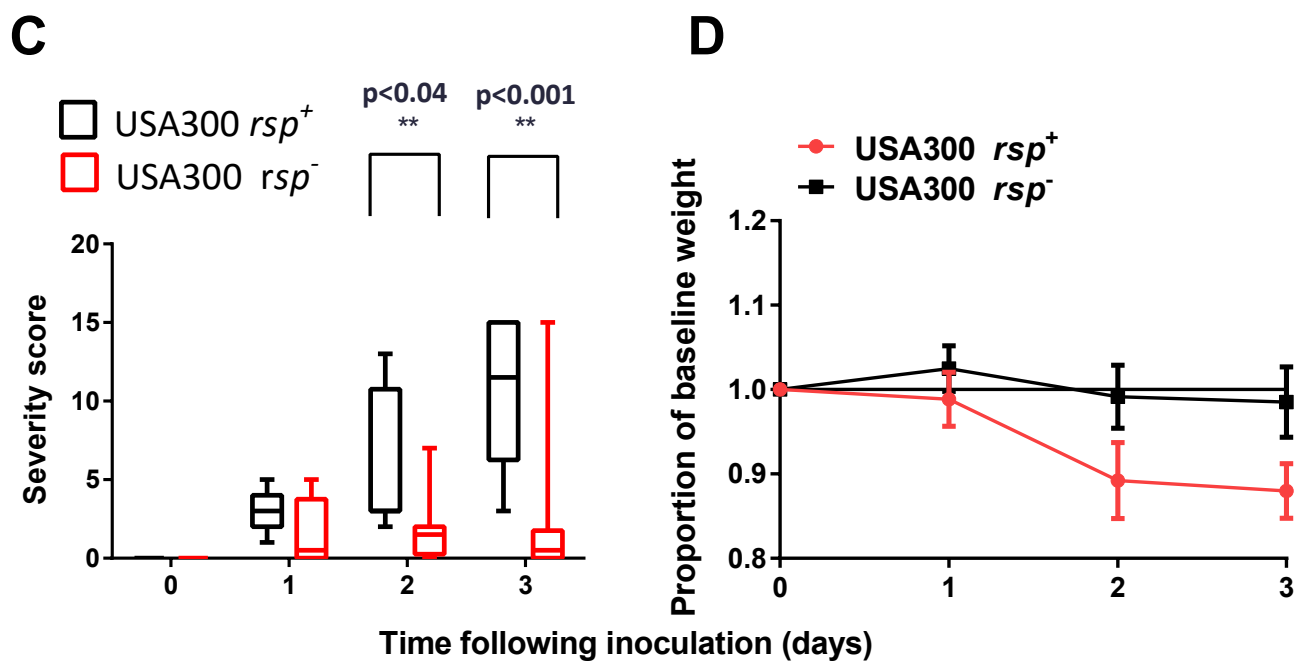
C
USA300 rsp+
USA300 rsp-
p<0.04
**
p<0.001
**
Severity score
20
15
10
5
0
0
1
2
3
D
USA300 rsp+
USA300 rsp-
Proportion of baseline weight
1.2
1.1
1.0
0.9
0.8
0
1
2
3
Time following inoculation (days)

Figure S4

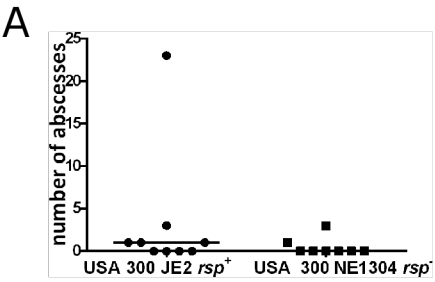
A
number of abscesses
25
20
15
10
5
0
USA 300 JE2 rsp+
USA 300 NE1304 rsp-

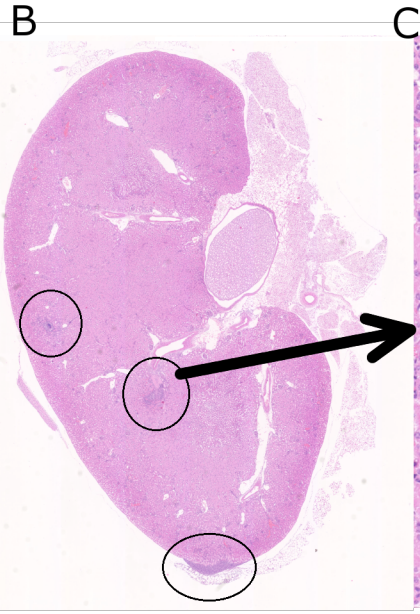
B

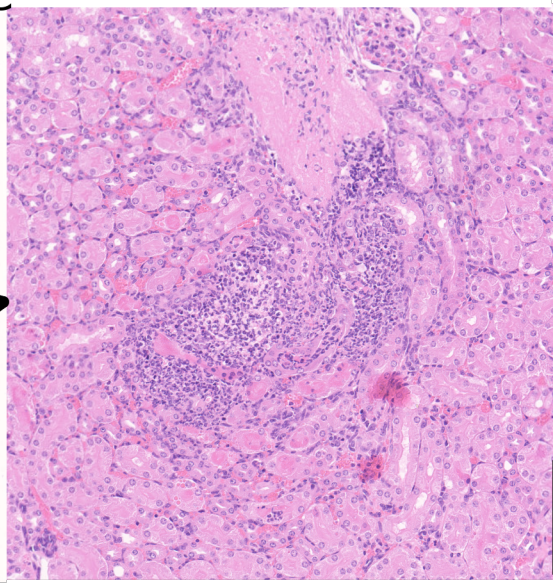
C


D

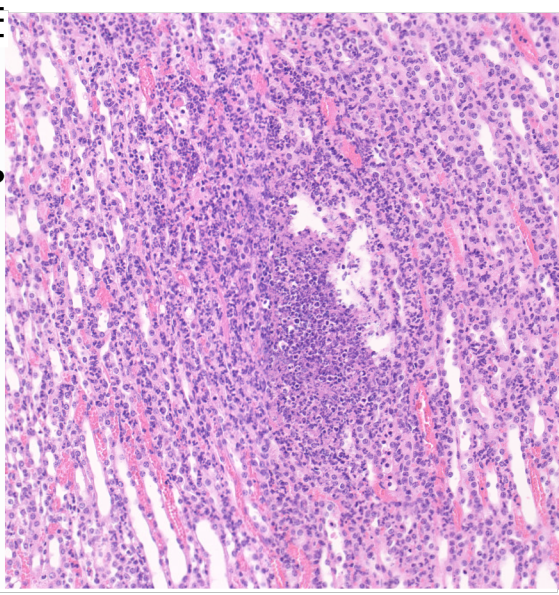
E

Patient S Patient P USA300

0.0
0.5
1.0
1.5
2.0
2.5

Figure S6

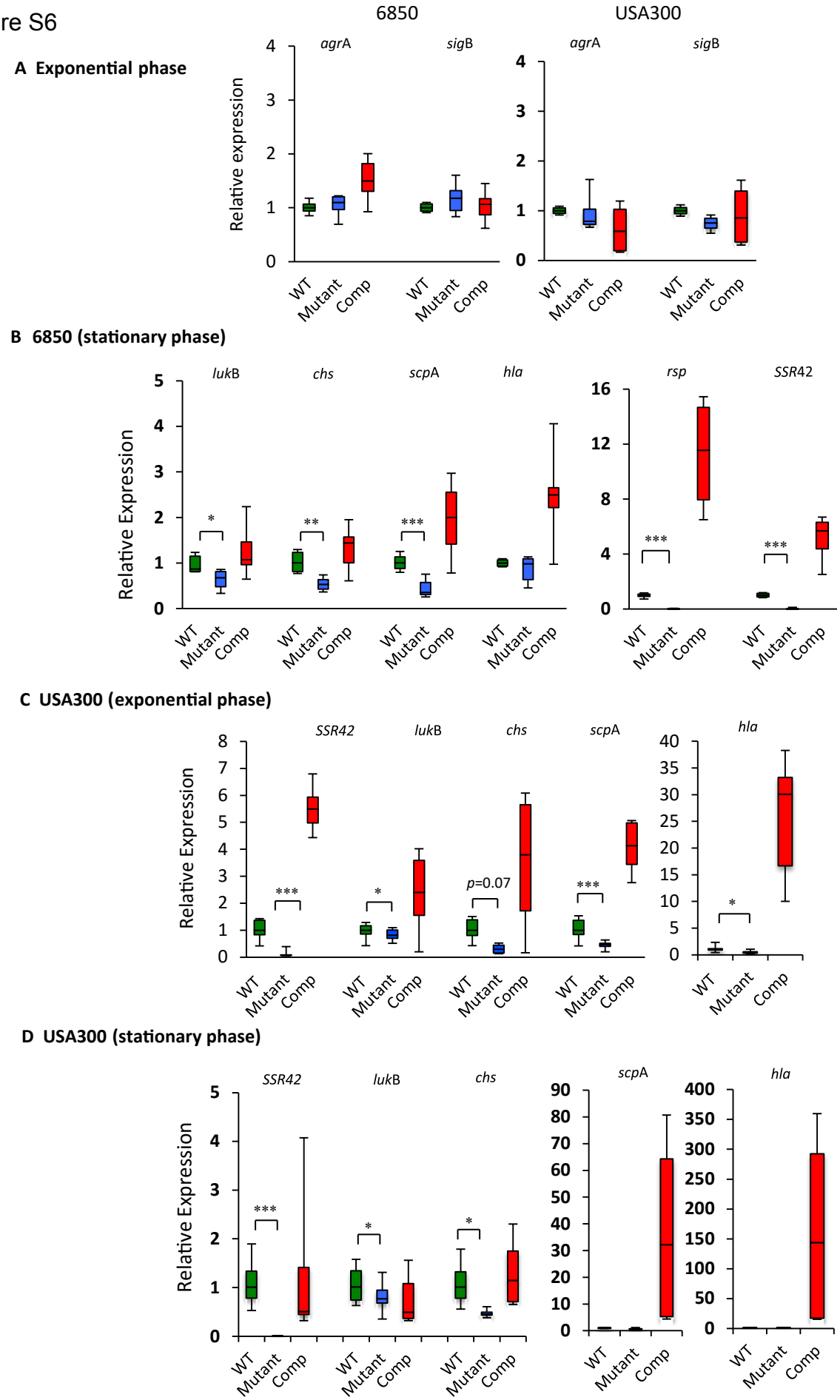
6850
USA300
A Exponential phase
agrA
sigB
Relative expression
WT
Mutant
Comp
B 6850 (stationary phase)
lukB
chs
scpA
hla
rsp
SSR42
Relative Expression
C USA300 (exponential phase)
p=0.07
D USA300 (stationary phase)

Figure S7

A

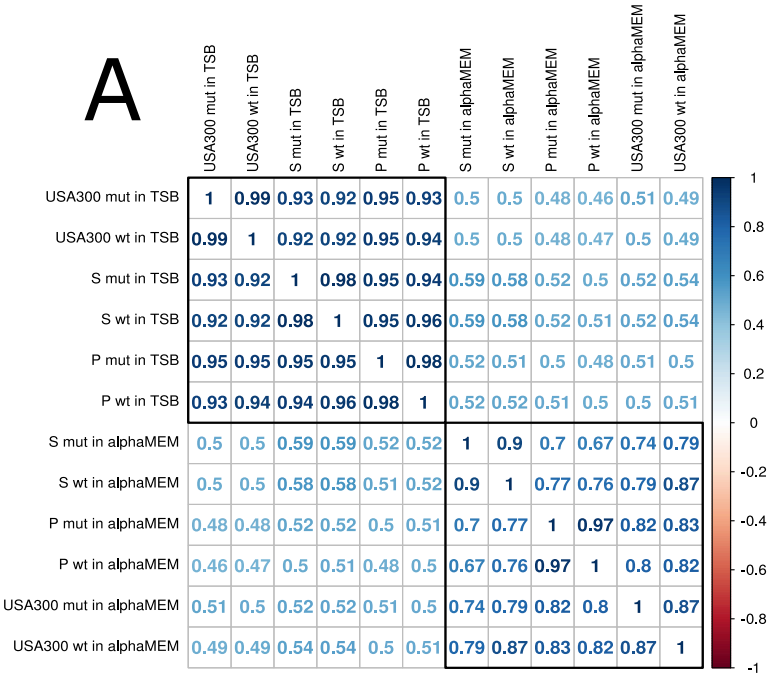
USA300 mut in TSB
USA300 wt in TSB
S mut in TSB
S wt in TSB
P mut in TSB
P wt in TSB
S mut in alphaMEM
S wt in alphaMEM
P mut in alphaMEM
P wt in alphaMEM
USA300 mut in alphaMEM
USA300 wt in alphaMEM
1 0.99 0.93 0.92 0.95 0.93 0.5 0.5 0.48 0.46 0.51 0.49
0.99 1 0.92 0.92 0.95 0.94 0.5 0.5 0.48 0.47 0.5 0.49
0.93 0.92 1 0.98 0.95 0.94 0.59 0.58 0.52 0.5 0.52 0.54
0.92 0.92 0.98 1 0.95 0.96 0.59 0.58 0.52 0.51 0.52 0.54
0.95 0.95 0.95 0.95 1 0.98 0.52 0.51 0.5 0.48 0.51 0.5
0.93 0.94 0.94 0.96 0.98 1 0.52 0.52 0.51 0.5 0.5 0.51
0.5 0.5 0.59 0.59 0.52 0.52 1 0.9 0.7 0.67 0.74 0.79
0.5 0.5 0.58 0.58 0.51 0.52 0.9 1 0.77 0.76 0.79 0.87
0.48 0.48 0.52 0.52 0.5 0.51 0.7 0.77 1 0.97 0.82 0.83
0.46 0.47 0.5 0.51 0.48 0.5 0.67 0.76 0.97 1 0.8 0.82
0.51 0.5 0.52 0.52 0.51 0.5 0.74 0.79 0.82 0.8 1 0.87
0.49 0.49 0.54 0.54 0.5 0.51 0.79 0.87 0.83 0.82 0.87 1
1
0.8
0.6
0.4
0.2
0
-0.2
-0.4
-0.6
-0.8
-1

B

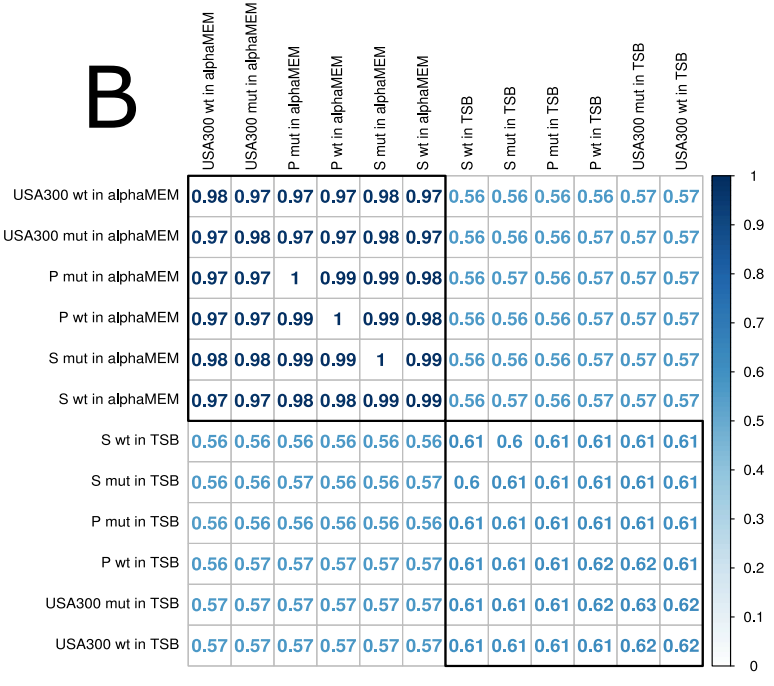
USA300 wt in alphaMEM
USA300 mut in alphaMEM
P mut in alphaMEM
P wt in alphaMEM
S mut in alphaMEM
S wt in alphaMEM
S wt in TSB
S mut in TSB
P mut in TSB
P wt in TSB
USA300 mut in TSB
USA300 wt in TSB
0.98 0.97 0.97 0.97 0.98 0.97 0.56 0.56 0.56 0.56 0.57 0.57
0.97 0.98 0.97 0.97 0.98 0.97 0.56 0.56 0.56 0.57 0.57 0.57
0.97 0.97 1 0.99 0.99 0.98 0.56 0.57 0.56 0.57 0.57 0.57
0.97 0.97 0.99 1 0.99 0.98 0.56 0.56 0.56 0.57 0.57 0.57
0.98 0.98 0.99 0.99 1 0.99 0.56 0.56 0.56 0.57 0.57 0.57
0.97 0.97 0.98 0.98 0.99 0.99 0.56 0.57 0.56 0.57 0.57 0.57
0.56 0.56 0.56 0.56 0.56 0.56 0.61 0.6 0.61 0.61 0.61 0.61
0.56 0.56 0.57 0.56 0.56 0.57 0.6 0.61 0.61 0.61 0.61 0.61
0.56 0.56 0.56 0.56 0.56 0.56 0.61 0.61 0.61 0.61 0.61 0.61
0.56 0.57 0.57 0.57 0.57 0.57 0.61 0.61 0.61 0.62 0.62 0.61
0.57 0.57 0.57 0.57 0.57 0.57 0.61 0.61 0.61 0.62 0.63 0.62
0.57 0.57 0.57 0.57 0.57 0.57 0.61 0.61 0.61 0.61 0.62 0.62
1
0.9
0.8
0.7
0.6
0.5
0.4
0.3
0.2
0.1
0

Figure S8

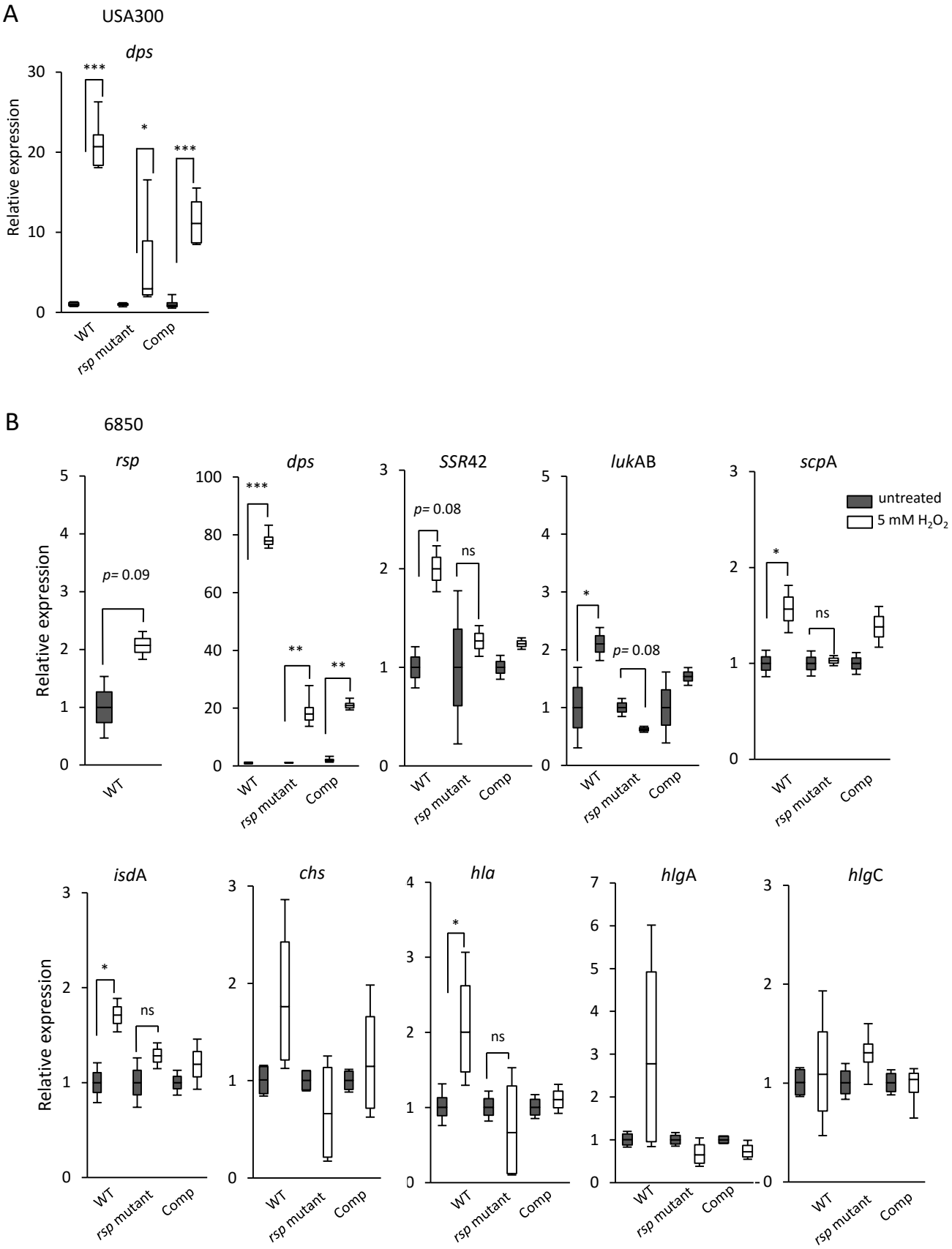
A
USA300
dps
Relative expression
WT
rsp mutant
Comp
B
6850
rsp
dps
SSR42
lukAB
scpA
untreated
5 mM H2O2
p= 0.09
p= 0.08
ns
isdA
chs
hla
hlgA
hlgC

Supplemental Tables

Supp. Table S1: Bacterial Strains used in this study[1]

Strain	Description	Source
Escherichia coli		
DH5α	*fhuA2 lac(del)U169 phoA glnV44 Φ80' lacZ(del)M15 gyrA96 recA1 relA1 endA1 thi-1 hsdR17*	Life technologies
TOP10F'	*F' [lacI^q Tn10(tet^R)] mcrA Δ(mrr-hsdRMS-mcrBC) φ80lacZΔM15 ΔlacX74 deoR nupG recA1 araD139 Δ(ara-leu)7697 galU galK rpsL(Str^R) endA1 λ$^-$*	Invitrogen™
Staphylococcus aureus		
RN4220	NCTC 8325-4 *sau1$^-$, hsdR$^-$*, non-hemolytic laboratory strain accepting foreign DNA	(1)
RN4220 pS2217	RN4220 with complementation plasmid p2217	This publication
6850	MSSA and β-lactam resistant *spa* type t185, sequence type 50 (2), Isolated from a patient with a skin abscess, progressed to bacteremia, osteomyelitis, septic arthritis, and multiple systemic abscesses	(3)
LAC	USA300 CA-MRSA, staphylococcal chromosomal cassette *mec* (SCC*mec*) type IV, *spa*-type 1, Sequence type 8 [ST8]. Fully sequenced, designated USA300_FPR3757. An epidemic community-acquired strain isolated from outbreaks of skin and soft tissue infections. It was also found in invasive disease, including severe septicemia, necrotizing pneumonia, and necrotizing fasciitis	(4-6)
JE2	USA300, *rsp$^+$*. Derivative of LAC, which was cured of three plasmids.	(7)
NE1304	NE1304, *rsp$^-$*, JE2 transposon insertion mutant within *rsp* gene, locus ID – SAUSA300_2326 (insertion at nucleotide 2501453, GenBank Accession NC_007793)	(7)
NE1532	JE2 transposon insertion mutant within *agr*A gene (locus ID SAUSA300_1992)	(7)
NE1622	JE2 transposon insertion mutant within *sae*R gene (locus ID SAUSA300_0691)	(7)
LAC* (AH1263)	USA300 CA-MRSA, Erythromycin-sensitive; Derivative of LAC cured of plasmid pUSA03	(8)
LAC* *rsp*::*ermB*	LAC*, phage-transduced recipient of NE1304 (Locus ID-SAUSA300_2326).	This publication
LAC* *rsp*::*ermB* pS2217	LAC* *rsp*::*ermB* complemented *in trans* for RSAU_002217 (*rsp* gene) with plasmid pS2217	This publication
6850 pBTn	6850 carrying plasmid pBTn (9) for transposon mutagenesis	This publication
6850 Δ2217	6850 *with* targeted deletion of gene locus RSAU_002217 (*rsp* gene) The complete open reading frame spanning from nucleotide 2353304 to 2355411 (GenBank Accession NC_022222) was deleted.	This publication
6850 Δ2217 pS2217	Complementation strain for locus RSAU_002217 (*rsp* gene) *in trans* with plasmid pS2217	This publication

Clinical isolates of *Staphylococcus aureus*		
Patient P nasal isolate	*rsp*$^+$ (Reference genome C1360, ST-15)	(10)
Patient P blood stream isolate	*rsp*$^-$, (Reference genome C11585, ST-15)	(10)
Patient S nasal isolate	*rsp*$^+$ (Reference genome C24365, ST-59)	This publication
Patient S blood stream isolate	*rsp*$^-$ (Reference genome C24366, ST-59)	This publication

[1]The references used in this table are listed in "Supplemental Table 1 References"

Supplemental Table 1 References

1. Recsei P, *et al.* (1986) Regulation of exoprotein gene expression in *Staphylococcus aureus* by agar. *Mol Gen Genet* 202(1):58-61.
2. Fraunholz M, *et al.* (2013) Complete Genome Sequence of *Staphylococcus aureus* 6850, a Highly Cytotoxic and Clinically Virulent Methicillin-Sensitive Strain with Distant Relatedness to Prototype Strains. *Genome announcements* 1(5).
3. Vann JM & Proctor RA (1987) Ingestion of *Staphylococcus aureus* by bovine endothelial cells results in time- and inoculum-dependent damage to endothelial cell monolayers. *Infect Immun* 55(9):2155-2163.
4. Pan ES, *et al.* (2003) Increasing prevalence of methicillin-resistant *Staphylococcus aureus* infection in California jails. *Clinical infectious diseases : an official publication of the Infectious Diseases Society of America* 37(10):1384-1388.
5. Diep BA, *et al.* (2006) Complete genome sequence of USA300, an epidemic clone of community-acquired meticillin-resistant *Staphylococcus aureus*. *Lancet* 367(9512):731-739.
6. Shopsin B, *et al.* (1999) Evaluation of protein A gene polymorphic region DNA sequencing for typing of *Staphylococcus aureus* strains. *Journal of clinical microbiology* 37(11):3556-3563.
7. Fey PD, *et al.* (2013) A genetic resource for rapid and comprehensive phenotype screening of nonessential *Staphylococcus aureus* genes. *mBio* 4(1):e00537-00512.
8. Boles BR, Thoendel M, Roth AJ, & Horswill AR (2010) Identification of genes involved in polysaccharide-independent *Staphylococcus aureus* biofilm formation. *PloS one* 5(4):e10146.
9. Li M, *et al.* (2009) *Staphylococcus aureus* mutant screen reveals interaction of the human antimicrobial peptide dermcidin with membrane phospholipids. *Antimicrobial agents and chemotherapy* 53(10):4200-4210.
10. Young BC, *et al.* (2012) Evolutionary dynamics of *Staphylococcus aureus* during progression from carriage to disease. *Proc Natl Acad Sci U S A* 109(12):4550-4555.

Supp. Table S2: Cloning and Adaptor Oligonucleotides

Name	Sequence (5'-3')
2217_intpromoter_F_NotI	GACAATGCGGCCGCCACTATTACCTTTTCAAAAATATTC
2217_intpromoter_R_BamHI	GATGTCGGATCCTTAGCTAGGTTTAAAGCAAATATATTTAAC
2217_test_F	ATATCTTGTTGCTGCTAATTC
2217_test_R	AACCGGAAATAGATTGACAC
2217-down-F-SacII	GATCGACCGCGGTAAATACTAACAGTCCTCTTGTGTTTAGTTT
2217-up-R-SacII	TCGATCCCGCGGATTTCTCTCTCCTGCCTAATATATATTGAAAT
attB1-2217-up-F	GGGGACAAGTTTGTACAAAAAAGCAGGCTTTGTTGTTGCACTATCTTGGTGA
attB2-2217-down-R	GGGGACCACTTTGTACAAGAAAGCTGGGTACGTTTTTCTCAATGCTTTCATCTT
MultiPlex-Y-Adapt_r	ACACTCTTTCCCTACACGACGCTCTTCCGATC*T
MultiPlex-Y-Adapt_f	[Phos]GATCGGAAGAGCACACGTCT
Himar_TnSeq_Read1_v2	ACCGAGATCTACGGACTTATCAGCCAACCTGT
MP-TnSeq_Index1	CAAGCAGAAGACGGCATACGAGATCGTGATGTGACTGGAGTTCAGACGTGTGCTCTTCCGATCT
MP-TnSeq_Index2	CAAGCAGAAGACGGCATACGAGATACATCGGTGACTGGAGTTCAGACGTGTGCTCTTCCGATCT
MP-TnSeq_Index6	CAAGCAGAAGACGGCATACGAGATATTGGCGTGACTGGAGTTCAGACGTGTGCTCTTCCGATCT
MP-TnSeq_Index7	CAAGCAGAAGACGGCATACGAGATGATCTGGTGACTGGAGTTCAGACGTGTGCTCTTCCGATCT
MP-TnSeq_Index8	CAAGCAGAAGACGGCATACGAGATTCAAGTGTGACTGGAGTTCAGACGTGTGCTCTTCCGATCT
MP-TnSeq_Index9	CAAGCAGAAGACGGCATACGAGATCTGATCGTGACTGGAGTTCAGACGTGTGCTCTTCCGATCT
MP-TnSeq_Index10	CAAGCAGAAGACGGCATACGAGATAAGCTAGTGACTGGAGTTCAGACGTGTGCTCTTCCGATCT
MP-TnSeq_Index11	CAAGCAGAAGACGGCATACGAGATGTAGCCGTGACTGGAGTTCAGACGTGTGCTCTTCCGATCT
MP-TnSeq_Index12	CAAGCAGAAGACGGCATACGAGATTACAAGGTGACTGGAGTTCAGACGTGTGCTCTTCCGATCT
MP-TnSeq_Index13	CAAGCAGAAGACGGCATACGAGATTTGACTGTGACTGGAGTTCAGACGTGTGCTCTTCCGATCT
MP-TnSeq_Index14	CAAGCAGAAGACGGCATACGAGATGGAACTGTGACTGGAGTTCAGACGTGTGCTCTTCCGATCT
MP-TnSeq_Index15	CAAGCAGAAGACGGCATACGAGATTGACATGTGACTGGAGTTCAGACGTGTGCTCTTCCGATCT
MP-TnSeq_Index16	CAAGCAGAAGACGGCATACGAGATGGACGGGTGACTGGAGTTCAGACGTGTGCTCTTCCGATCT
MP-TnSeq_Index17	CAAGCAGAAGACGGCATACGAGATCTCTACGTGACTGGAGTTCAGACGTGTGCTCTTCCGATCT
TnSeq-HimarPCR_v2-PT	GACCACCGAGATCTACGAGACCGGGGACTTATCAGC
himar-5-PCR	CCATAACTTTAGGGTTAACCATACGC
himar-3-PCR	CAGCTTCCAAGGAGCTAAAGAGGTCC
IS-Himar-forward	AATGATACGGCGACCACCGAGATCT
IS-BC-Reverse	CAAGCAGAAGACGGCATACGAGAT

Supp. Table S3: Real-time RT-PCR Oligonucleotides

Name	Sequence	target
RT-agrA-R	GTTACCAACTGGATCATGCT	*agr*A
RT-agrA-F	TATGAGGTGCTTGAGCAAG	*agr*A
RT-CHIPS-R	ATCAGTACACACCATCATTCAG	*chs*
RT-CHIPS-F	ATCAGTACACACCATCATTCAG	*chs*
RT-dps-R	TTAATGTACCTACAGGGTTTCC	*dps*
RT-dps-F	AATCAACAAGTAGCAAACTGG	*dps*
RT-gyrB-R	ATAGCCTGCTTCAATTAACG	*gyr*B
RT-gyrB-F	CGACTTTGATCTAGCGAAAG	*gyr*B
RT-hla-R	CAATTTGTTGAAGTCCAATG	*hla*
RT-hla-F	GATCCTAACAAAGCAAGTTCTC	*hla*
RT-hlgC-R	TGATCCATTACCACCGAGT	*hlg*C
RT-hlgC-F	ATCTACAAACGTGAGTCAGACA	*hlg*C
RT-hlgA-R	TGATGATTTCTGCACCTTG	*hlg*A
RT-hlgA-F	CCTTTAGCCAATCCATTTATAG	*hlg*A
RT-lukS-PV-R	TCCTGTTGATGGACCACT	*luk*S
RT-lukS-PV-F	GTGGCCTTTCCAATACAATA	*luk*S
RT-isdA-R	GTATTCTTTCCAGAATGATGC	*isd*A
RT-isdA- F	GCTACGAACGCAACTAATAATC	*isd*A
RT-lukG-R	GATTAAACCCTTCAGACACAGT	*luk*G
RT-lukG-F	CATGACCATACGAGACAATTAAC	*luk*G
RT-lukH-R	CTTGAAAATCTACATGGTACTCAC	*luk*H
RT-lukH-F	CAATTCGACTTTATCGATGAT	*luk*H
RT-2217-R	GACTTCGATCTTTCGGATT	*rsp*
RT-2217-F	TTCACTCGTTTCCAAGATTAC	*rsp*
RT-scpA-R	GGTTCACCAAGTGTATACGAG	*scp*A
RT-scpA-F	TTAATGTCGAGGACAAGAGTG	*scp*A
RT-sigB-R	GGCCCAATTTCTTTAATACG	*sig*B
RT-sigB-F	CTTTGAACGGAAGTTTGAAG	*sig*B
RT-SSR42-R	CACCTAACATCAAAGAATATTCATC	*ssr*42
RT-SSR42-F	TATCTTGTTGCTGCTAATTCTATTG	*ssr*42

Supp. Table S4: Scoring system used for mice challenged intravenously with *S. aureus*

	Description	Score
Appearance	Normal	0
	General lack of grooming	1
	Coat staring, ocular and nasal discharges	2
	Piloerection, hunched up	3 – endpoint
Behavior	Normal	0
	Slight change; either less or more active than usual	1
	Agitated, alert, isolated or significantly less mobile	2
	Vocalisation, self-mutilation, unusual aggression or stillness	3 - endpoint
Mouse grimace score*	Orbital tightening	0-1-2
	Nose and/or cheek bulge	0-1-2
	Ear position	0-1-2
Arthropathy+	Normal	0
	Decreased movements	1
	Decreased movements and either swelling of joints or nodose tail	2
	Decrease movements and retracted limb	3 - endpoint
Total score		0-24

**According to Langford, D.J., et al., Coding of facial expressions of pain in the laboratory mouse. Nature Methods, 7, 447–449 (2010). +The arthritis scoring system is based on the known manifestations of S. aureus arthritis as described in a series of papers by Tarkowski A and colleagues, e.g Bremell T et al 1995 Infection & Immunity 63: 4185; Bremell T 1992 Infection & Immunity 60: 2976.*